A Light-Dependent Mechanism for Massive Accumulation of Manganese in the Photosynthetic Bacterium Synechocystis sp. PCC 6803 †

ARTICLE *in* BIOCHEMISTRY · JANUARY 2003

Impact Factor: 3.02 · DOI: 10.1021/bi026892s · Source: PubMed

4 AUTHORS, INCLUDING:

Nir Keren
Hebrew University of Jerusalem
56 PUBLICATIONS **1,514** CITATIONS
SEE PROFILE

James Penner-Hahn
University of Michigan
272 PUBLICATIONS **10,045** CITATIONS
SEE PROFILE

A Light-Dependent Mechanism for Massive Accumulation of Manganese in the Photosynthetic Bacterium *Synechocystis* sp. PCC 6803†

Nir Keren,*,‡ Matthew J. Kidd,§ James E. Penner-Hahn,§ and Himadri B. Pakrasi‡

Department of Biology, Washington University, St. Louis, Missouri 63130-4899, and Department of Chemistry and Biophysics Research Division, The University of Michigan, Ann Arbor, Michigan 48109-1055

Received September 23, 2002; Revised Manuscript Received October 22, 2002

ABSTRACT: Manganese is an essential micronutrient for many organisms. Because of its unique role in the water oxidizing activity of photosystem II, manganese is required for photosynthetic growth in plants and cyanobacteria. Here we report on the mechanism of manganese uptake in the cyanobacterium *Synechocystis* sp. PCC 6803. Cells grown in 9 μM manganese-containing medium accumulate up to 1×10^8 manganese atoms/cell, bound to the outer membrane (pool A). This pool could be released by EDTA treatment. Accumulation of manganese in pool A was energized by photosynthetic electron flow. Moreover, collapsing the membrane potential resulted in the immediate release of this manganese pool. The manganese in this pool is mainly Mn(II) in a six-coordinate distorted environment. A distinctly different pool of manganese, pool B ($\sim 1.5 \times 10^6$ atoms/cell), could not be extracted by EDTA. Transport into pool B was light-independent and could be detected only under limiting manganese concentrations (1 nM). Evidently, manganese uptake in *Synechocystis* 6803 cells occurs in two steps. First, manganese accumulates in the outer membrane (pool A) in a membrane potential-dependent process. Next, manganese is transported through the inner membrane into pool B. We propose that pool A serves as a store that allows the cells to overcome transient limitations in manganese in the environment.

Transition metal ions are essential as cofactors in most cellular processes. Tight regulation of transport and control of homeostasis are needed to ensure that adequate amounts of transition metals are present in the cell (*1*). A series of membrane-bound transporters facilitate the transport of transition metal ions into the cell. Once inside the cell, the metals are ligated by chaperone molecules that direct them to their final destination (*2*). Very little, if any, free transition metal can be found inside the cell. In the oxidative environment of the cells, free transition metals can undergo redox reactions that produce harmful oxygen species (*3*, *4*). Systems for transport and accumulation of iron, zinc, copper, and magnesium in bacteria have been thoroughly investigated (*4*−*6*). However, the details of the transport and accumulation mechanisms for manganese, which is essential as a cofactor for a large number of enzymes, have begun to emerge only recently (*7*).

Efficient control of the internal manganese concentration is essential for cellular metabolism and for protection against active oxygen species. Manganese serves as a cofactor for one of the superoxide dismutases, a key enzyme in the active oxygen species detoxifying pathway (*3*). Indeed, mutations that inactivate manganese transporters affect the virulence of a number of bacteria, including members of the *Streptococcus* and *Enterococcus* genera (*7*). In *Streptococcus pneumoniae*, a decreased level of manganese transport has been correlated with enhanced sensitivity to oxidative stress (*8*).

High-affinity manganese transporters have been described in a series of earlier studies on a number of bacteria, including *Escherichia coli* (*9*), *Bacillus subtilis* (*10*), *Staphylococcus aureus* (*11*), and the photosynthetic bacteria *Rhodopseudomonas capsulatus* (*12*) and *Anacystis nidulans* (*13*). In general, manganese transport activities were inhibited by respiration inhibitors and uncouplers, suggesting an energy-dependent transport process (*14*). Transport of manganese is mediated by specific transporters that belong to a number of families (*15*). So far, manganese transporters of the ABC, Nramp, and P-type ATPase families have been described in several bacterial species.

In oxygenic photosynthetic organisms, manganese plays a unique role. It is required during water splitting on the electron donor side of photosystem II (PSII)[1] (*16*). In this process, two water molecules are oxidized, oxygen is released, and four electrons are transferred to two plastoquinone molecules. The site of catalysis is composed of four manganese ions, one calcium ion, and one chloride ion (*17*).

† This study was supported by grants from USDA-NRI Department of Energy, and the Department of Biology, Washington University, from funds provided by the Danforth Foundation to H.B.P., and by National Institutes of Health Grant GM-45205 to J.E.P.-H. N.K. was supported by the International Human Frontier Science Program and The European Molecular Biology Organization. The SSRL is supported by the U.S. Department of Energy with additional support from the NIH Research Resource program.

* To whom correspondence should be addressed: Department of Biology, Campus Box 1137, Washington University, One Brookings Drive, St. Louis, MO 63130-4899. Telephone: (314) 935-6862. Fax: (314) 935-6803. E-mail: nir@biology2.wustl.edu.

‡ Washington University.

§ The University of Michigan.

[1] Abbreviations: EDTA, ethylene-diamine-tetraacetic acid; CCCP, carbonyl cyanide *m*-chlorophenylhydrazone; DCMU, 3-(3,4-dichlorophenyl)-1,1-dimethylurea; EXAFS, extended X-ray absorption fine structure; XANES, X-ray absorption near-edge structure; XAS, X-ray absorption spectroscopy; PSII, photosystem II.

10.1021/bi026892s CCC: $22.00
Published on Web 11/20/2002

Synechocystis sp. PCC 6803, a free-living freshwater cyanobacterium, has been used extensively as a model organism for the study of photosynthetic processes. It is a Gram-negative bacterium with an outer and inner membrane, defining the envelope layer of the cell, and an internal thylakoid membrane system in which photosynthetic electron transfer reactions occur (*18*). In *Synechocystis* 6803, MntABC, an ABC-type transporter for Mn, was identified in a screen for photosynthesis-deficient mutants (*19*). This transporter is functional in cells grown under manganese-starved conditions, and is not essential for photoautotrophic growth under manganese-sufficient conditions (9 μM). Evidently, *Synechocystis* 6803 cells have additional manganese transport systems (*20*), which are yet to be identified at a molecular level.

In this work, we have begun to dissect the complexity of the manganese uptake system in this photosynthetic organism by measuring the concentrations of manganese transported into the cell under various environmental conditions. We have identified two pools of manganese in cyanobacterial cells: pool A, which can be released by EDTA, and pool B, which cannot be extracted by this metal chelator. On the basis of the properties of the transport of manganese into the two pools, we propose a two-step mechanism of transport. The first is transport into pool A, located in the outer membrane, in a light-dependent manner. The second step is transport through the inner membrane into pool B.

EXPERIMENTAL PROCEDURES

Cell Growth and Preparation. Synechocystis 6803 cells were grown in normal BG11 medium (*21*) or on BG11 medium without added manganese (BG11-Mn). The Δ*mntC* mutant, in which the gene for the MntC subunit of the MntABC transporter had been inactivated (*20*), was grown on BG11 medium containing 10 μg/mL kanamycin. The concentration of manganese was 9 μM in normal BG11 medium and 1 nM in BG11-Mn. Cultures were grown in glass tubes, 3 cm in diameter, with constant air bubbling at 30 °C. The light intensity was adjusted to 100 μmol photons m^{-2} s^{-1}. Cultures were maintained continuously in BG11 or BG11-Mn and diluted daily. The cels density was measured as OD_{730} on a DW2000 spectrophotometer (SLM-Aminco, Urbana, IL). A calibration of OD_{730} to cell number, measured with a hemocytometer (American Optical Corp., Buffalo, NY), was used to calculate the concentration of cells from OD_{730} in the different experiments ($OD_{730} = 1.9 \times 10^9$ cells/mL). All of the cultures that were used had an OD_{730} of >0.15. Under our growth conditions, cultures were in the logarithmic phase until they reached an OD_{730} of 0.4.

In preparation for metal ion accumulation experiments, cells were harvested by centrifugation for 5 min at 3000*g*. To remove excess metal ions from the culture medium, the cells were washed and resuspended three times in 20 mM HEPES (pH 7.8) and concentrated to an OD_{730} of 2−3.

Membrane Isolation and Fractionation. For membrane isolation, cells were broken by glass beads, as previously described (*22*). Pelleted cells were resuspended in 1 mL of HEPES buffer (20 mM, pH 7.8) and mixed with 0.18 mm diameter glass beads. The cells were shaken with the glass beads for 1 min using a vortex mixer at room temperature. Unbroken cells were removed by centrifugation for 5 min at 6000*g*. Using this procedure, >90% of the cells were broken. The membrane mixture, containing thylakoid, inner, and outer membranes, was separated from the soluble fraction by centrifugation at 540000*g* for 5 min at 25 °C in a TL-100 tabletop ultracentrifuge (Beckman, Palo Alto, CA). To separate the different membrane components from this mixture, the procedure described in ref *23* was used with modifications. Membranes were loaded on a 10 to 50% (w/v) sucrose gradient in a buffer containing 20 mM HEPES (pH 7.8) and 0.04% Triton X-100. The gradient was spun at 300000*g* in a T-865 rotor (Sorval, Newton, MA) for 3 h at 10 °C. One milliliter fractions were collected from the bottom to the top of the gradient.

Metal Content Measurements by Atomic Absorption Spectrophotometry. Kinetic manganese uptake experiments were performed in glass tubes, 2 cm in diameter, set in a water bath at 32 °C. Illumination was provided by an Oriel 6687 projector (Oriel Scientific, Surrey, England). A light intensity of 500 μmol photons m^{-2} s^{-1} was used for all experiments.

At the start of the experiment, concentrated cells were diluted to a final concentration of 0.1 OD_{730} into BG11 or BG11-Mn medium as indicated in the figure legends. Four milliliter samples were collected at the indicated times and immediately spun down by momentary centrifugation in an HB-4 (Sorval) rotor at 15000*g*. A sample of the medium was collected. The cell pellet was resuspended in 8 mL of EDTA wash buffer [20 mM HEPES (pH 7.8) and 5 mM EDTA]. The sample was centrifuged again at the same speed, and a sample of the EDTA wash buffer was collected. The pellet containing the cells was resuspended in 8 mL of 80% nitric acid.

To determine the initial rate of transport, 1 mL samples were centrifuged for 1 min in a tabletop microcentrifuge at 16000*g* to sediment the cells. Samples of the cell-free medium were collected for analysis.

All of the solutions and samples used in the experiments were kept in plastic containers or in acid-washed glass vessels to avoid metal contamination. Metal concentrations in the medium, EDTA wash, and nitric acid-digested cells were measured on an AA600 atomic absorption spectrophotometer (Perkin-Elmer, Ueberlingen, Germany). Sucrose gradient samples were measured in a 90% nitric acid solution. Each measurement was repeated three times. The standard deviations for all the data presented were less then 5% of the average value.

Manganese Uptake Measurements with $^{54}Mn^{2+}$. Cells grown in BG11-Mn medium were harvested and resuspended to a final concentration of 0.1 OD_{730} in 1 cm diameter glass tubes maintained at 30 °C in BG11-Mn medium. The light intensity for the experiments was 30 μmol photons m^{-2} s^{-1}. At the beginning of the experiment, carrier-free $^{54}MnCl_2$ (Perkin-Elmer, North Billerica, MA) was added to the medium to a final concentration of 1 μCi/mL (equivalent to 1 nM manganese). At various times, 50 μL samples were diluted into 5 mL of either 10 mM $MnCl_2$ or EDTA wash buffer, as indicated. The samples were filtered onto nitrocellulose filters that were measured for radioactivity on a LS5000 TD scintillation counter (Beckman). Each time point was repeated in triplicate. The standard deviations were ≤15% of the average value for all of the data presented.

X-ray Absorption Measurements. Samples for X-ray absorption measurements were prepared from cells grown

on BG11 medium. Cells were harvested by centrifugation for 5 min at 3000*g* and resuspended in 20 mM HEPES (pH 7.8). This sample was packed into a Lucite cuvette (2 mm × 2 mm × 25 mm sample volume) covered with a 20 μm polypropylene front window. All sample preparation was completed in the light. The sample was then frozen in dry ice for shipment to the Stanford Synchrotron Radiation Laboratory (SSRL).

X-ray absorption data were measured on beamline 7-3 at the SSRL using a Si(220) double-crystal monochromator detuned 50% for harmonic reduction. Energies were calibrated by measuring the absorption spectrum of $KMnO_4$ as an internal standard and defining the energy of the pre-edge peak for $KMnO_4$ as 6543.3 eV. The sample was held at 11 K during measurements using a liquid helium flow cryostat. Data were measured as fluorescence excitation spectra using a 30-element intrinsic Ge solid-state fluorescence detector. The incident count rate was held at less than 50 000 s^{-1} to prevent detector saturation, giving a useful count rate of ca. 2000 s^{-1} per channel. Spectra were measured using 5 eV steps in the pre-edge region, 0.4 eV steps in the edge region, and 0.05 $Å^{-1}$ steps in the extended X-ray absorption fine structure (EXAFS) region to a k of 11.5 $Å^{-1}$, the upper limit set by the presence of iron in the samples. Integration times for the three regions were 1 s, 1 s, and k^3-weighted times from 1 to 25 s, respectively, for a total measurement time of ca. 30 min/scan, giving a total of ca. 1.4×10^6 useful counts per point at $k = 11.5$ $Å^{-1}$. Eight scans were measured and averaged to generate the final spectrum.

X-ray absorption near edge structure (XANES) data were normalized by using a single polynomial background and a single scale factor to maximize the agreement, both well below and well above the edge, with the McMaster X-ray absorption cross sections (*24*). EXAFS data reduction used a first-order polynomial in the pre-edge and a two-region cubic spline through the EXAFS data. Data were converted to k space using E_0 and 6545 eV and were fit using G.I.FEFFIT (*25*, *26*) using amplitude and phase functions calculated with Feff version 6.0 (*27*−*29*). Fits to both Fourier-filtered ($R = 0.9-3.0$ Å) and unfiltered data gave equivalent structural parameters. A scale factor of 0.89 and a ΔE_0 of 7 eV were defined by fitting the EXAFS data for hexaquo Mn(II) and used for fitting the biological data.

RESULTS

Two Distinct Pools of Manganese in Synechocystis 6803 Cells. To determine the total amount of manganese in *Synechocystis* 6803 cells, we have used a sensitive atomic absorption spectroscopic technique. In wild-type cells diluted in fresh BG11 medium 1 day before the experiment, only a small fraction (≈2.7%) of the manganese remained in the medium after centrifugation to remove the cells, while the bulk of the manganese sedimented with the cells (Figure 1A). However, ≈97.6% of the manganese bound to the cells could be washed away. While ≈22.5% of the bound manganese was released by wash with a buffer without EDTA, and can be considered loosely bound, ≈75.1% could be released only when EDTA was added to the wash buffer. This latter fraction will be termed "pool A" manganese, while the manganese that remained associated with the cells after the EDTA wash (≈2.4%) will be termed "pool B" manganese.

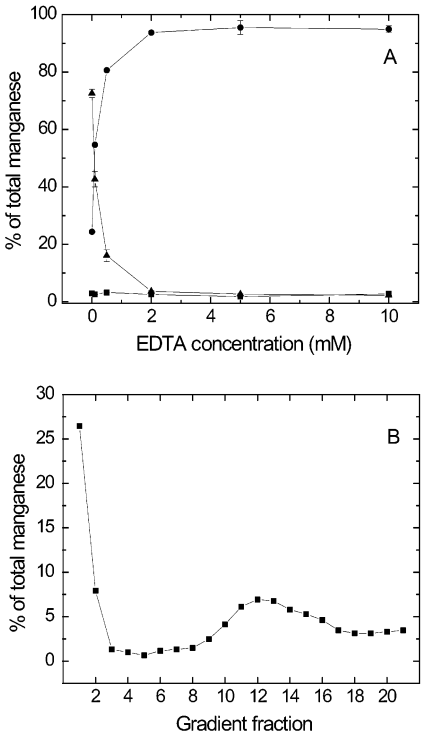

FIGURE 1: EDTA washable manganese pool in *Synechocystis* 6803. (A) Samples of cells, at a concentration of 2×10^8 cells/mL, were washed with a buffer containing various concentrations of Na_2EDTA. Concentrations of manganese are shown as percent fractions of the total (5.5 μM): (■) in the medium, (●) in the EDTA wash buffer (pool A), and (▲) in EDTA-washed cells (pool B). Error bars represent standard errors from three replicate measurements. (B) Cellular membranes were fractionated on a 10 to 50% sucrose gradient. Fractions were collected from the bottom of the gradient upward. Fraction 1 contained the pelleted material.

Under our experimental conditions, the ability to wash away manganese with EDTA was saturated between 2 and 5 mM. An EDTA concentration of 5 mM was selected for washing in the following experiments. While the stability constant for the binding of manganese to EDTA is high [log $K_1 = 13.8$ M^{-1} (*30*)], a large concentration was needed because of the masking effect of other cations in the medium. EDTA can chelate various cations from the exterior as well as from the envelope layer of the cells, because of its ability to porate the outer membrane of Gram-negative bacteria (*31*). EDTA treatment has been shown to be effective in releasing periplasmic proteins from *Synechocystis* 6803 (*32*) and *Synechococcus* sp. WH 7803 (*33*). Since EDTA cannot penetrate the inner membrane, pool A most probably represents the manganese in the envelope layer. Pool B represents manganese that has been transported across the inner membrane into the cytoplasm or manganese that is bound to the cell with an affinity higher than that of EDTA.

To localize pool A to a cellular compartment, we have fractionated the cells into soluble and membrane phases after breakage with glass beads. This method results in the formation of mainly right-side-out membrane vesicles (*22*). As compared to control cells that were treated identically but not broken with glass beads, 76.5 ± 9.5% ($n = 4$) of the manganese in the EDTA washable pool A sedimented with the membrane fraction in centrifugation.

The membrane fraction is a mixture of thylakoid, inner, and outer membranes that can be separated by sucrose

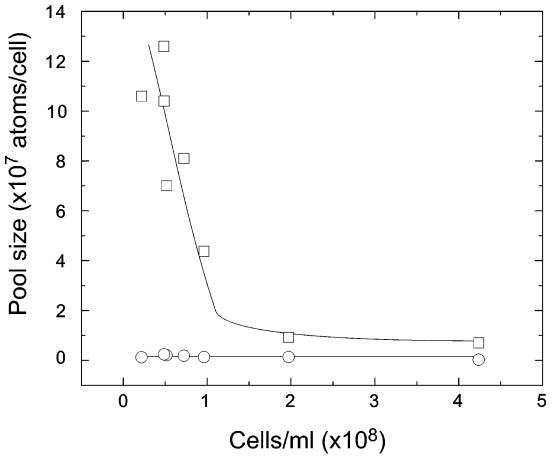

FIGURE 2: Size of pools A and B as a function of the cell density in the culture. Wild-type *Synechocystis* 6803 cells grown in normal BG11 medium were harvested at different culture densities, as indicated on the *x*-axis, and the sizes of the EDTA washable pool A (□) and the nonwashable pool B (○) were determined.

gradient centrifugation (*23*). In the gradient presented in Figure 1B, the outer membrane was collected in the pellet (fraction 1), the thylakoid membrane in fractions 10−14, and the plasma membrane in fractions 14−17. The distribution of manganese in the gradient indicates that a majority of the manganese bound to the membrane fraction was associated with the outer membrane. Therefore, pool A is most probably bound to the outer membrane.

Size of Pool A and Pool B. Large amounts of manganese accumulate in pool A. As shown in Figure 2, young cultures accumulated manganese at an excess of up to 80-fold in pool A as compared to pool B. When the cells divided and the density of the culture increased, the manganese from pool A was utilized and the size of this pool decreased. The size of pool B, on the other hand, was tightly regulated and did not change as a function of cell density. The average size of pool B was $1.5 \times 10^6 \pm 7.1 \times 10^5$ atoms/cell ($n = 7$). However, in cells grown in the manganese poor BG11-Mn medium, the size of pool B was $2.1 \times 10^5 \pm 1.2 \times 10^5$ atoms/cell ($n = 4$), 7 times smaller than in cells grown in BG11 medium.

Molecular Properties of Pool A Manganese. The XANES spectrum for the frozen cells is shown in Figure 3, with the corresponding spectrum for hexaquo Mn(II) shown for comparison. The whole-cell spectrum is the weighted average of the spectra for the manganese in pools A and B. However, since 98% of the manganese is in pool A, this spectrum is effectively that of the pool A manganese. The low energy of the absorption edge indicates that the manganese in pool A is present predominantly as Mn(II), and this was confirmed by fitting the data with a mixture of manganese reference compounds (*34*). No significant improvement in fit quality was observed when Mn(III) or Mn(IV) models were included in the fit. Although the manganese is clearly present as Mn(II), the intensity of the peak at ca. 6555 eV for the frozen cells is significantly lower in magnitude than that seen for hexaquo Mn(II), and the peak is significantly broader. This is very similar to results seen in Mn(II) model compounds and in binuclear Mn(II) proteins (*35*) when the manganese is present in a distorted, nonoctahedral, coordination environment. Consistent with this, the area of the 1s → 3d transition for the cells, 27 eV cm^2 g^{-1}, is approximately 35% larger

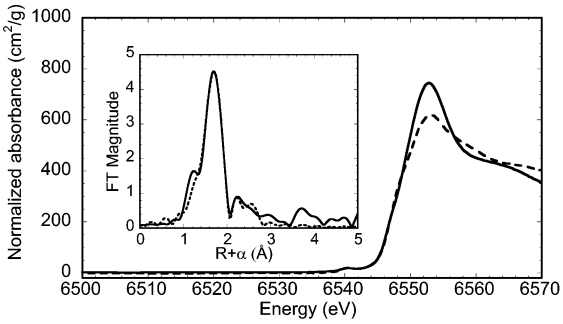

FIGURE 3: *Synechocystis* 6803 whole-cell XANES spectrum. Normalized XANES spectra for frozen cells (—) and Mn(II)$(H_2O)_6$ (- - -). The inset shows the Fourier transform (—) and the best fit using an Mn−O shell and an Mn−C shell (- - -) as described in the text, for whole-cell EXAFS. EXAFS data were k^3 weighted and Fourier transformed over the range of 2−11.5 Å^{-1}. The culture used for the experiment had a density of 2.2×10^7 cells/mL. The ratio of manganese in pool A:pool B was 84.8.

that that seen for octahedrally symmetric complexes, but typical of that seen for distorted six-coordinate manganese models (*35*).

The Fourier transform of the EXAFS data is shown in the inset of Figure 3. The data are dominated by scattering from only a single nearest neighbor, and can be modeled well using only a single shell of Mn−O/N scattering, with an apparent Mn−O distance of 2.18 Å. The absence of significant outer shell peaks at $R + \alpha$ values of ≈3 and ≈4 Å indicates that the manganese in pool A is not coordinated primarily to histidine ligands, although the weak outer shell scattering would be consistent with coordination by an average of one or perhaps even two histidine ligands per manganese (*35*). There is a small outer shell peak on the high-*R* side of the main peak. This can be modeled well as a shell of C atoms at 3.13 Å. The presence of a low-*Z* scatterer at ca. 3 Å is consistent with coordination by one or more protein-derived ligands since the 3.1 Å low-*Z* shell could arise from, for example, the carbon atoms of carboxylate ligands. Given the high local concentration of manganese, it is possible that the manganese is present as an oligomer of some sort. There is no evidence for outer shell scattering that can be attributed to Mn−Mn interactions. However, this does not rule out the possibility of a multinuclear manganese assembly, since weak, disordered Mn dimers do not give readily detectable Mn−Mn interactions (*35*).

The average Mn−O/N distance is consistent with a six-coordinate Mn. If there were a significant fraction of five-coordinate manganese, the average distance would be shorter, since the average Mn−O distance for five-coordinate manganese is ca. 2.10 Å (*36*). Despite the long Mn−O distance, the apparent manganese coordination number was only 4. The long Mn−O distance and the relatively small 1s → 3d amplitude both rule out the possibility that the manganese is four-coordinate. Rather, the anomalously small coordination number and relatively large Debye−Waller factor (8×10^{-3} Å^2) are typical of fits that are found for authentic distorted six-coordinate Mn(II) (*35*). The EXAFS and XANES data thus both suggest that the manganese must be present in a distorted site. Although it is likely that the manganese is coordinated to a mixture of oxygen and nitrogen ligands, the data presented here do not justify fits using multiple shells.

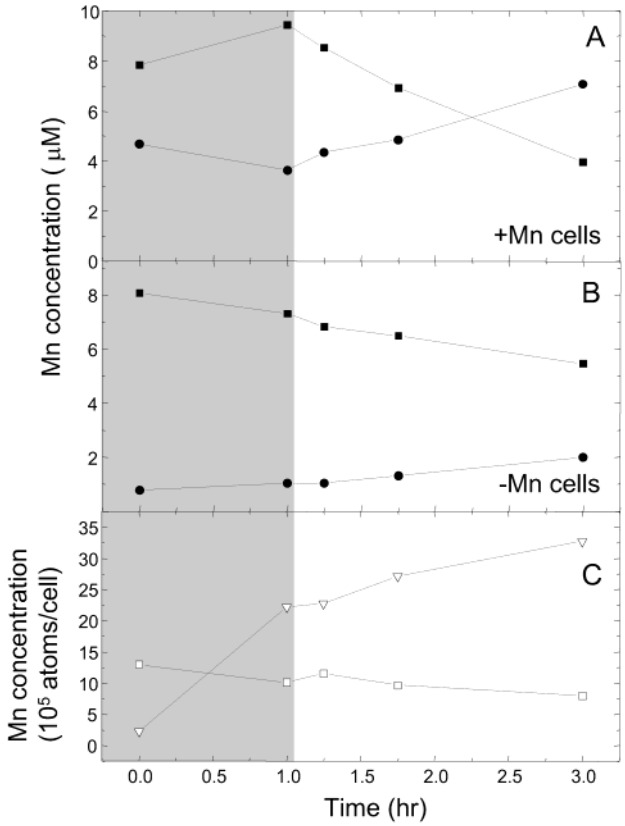

FIGURE 4: Time course of manganese accumulation. Wild-type *Synechocystis* 6803 cells, grown in normal (A) or BG11-Mn medium (B), were tested for the kinetics of manganese accumulation in the dark and in the light. The shaded areas represent dark incubation: (■) manganese concentration in the medium and (●) manganese concentration in pool A. Since manganese concentrations in pool B were much lower than in the medium and in pool A, they are presented separately in panel C: (▽) cells grown in BG11-Mn medium and (□) cells grown in BG11 medium.

Light Dependence of Manganese Accumulation. Since manganese is essential for photosynthetic activity, it was of interest to determine the effect of light on the accumulation of manganese. In the experiments presented in Figure 4, we have measured the kinetics of manganese uptake by measuring its concentration in the medium, pool A, and pool B as a function of time and illumination.

Accumulation of manganese in pool A was observed only in the light. The rate of accumulation varied between experiments depending on the physiological state of the cells and the initial size of the pool. However, the extent of accumulation in this pool was much larger in cells grown on BG11 than in cells grown on BG11-Mn (Figure 4A,B). Some release of manganese from this pool to the medium occurred in the dark (Figure 4A). The fast accumulation of manganese in the light and the slow release in the dark were independent of the order of the light and dark periods (data not shown). Accumulation of manganese in pool B could be detected only in cells starved for manganese during growth in BG11-Mn, and was light-independent (Figure 4C).

Uptake of Trace Amounts of Radioactive Manganese. Previous studies on the kinetics of manganese transport in bacterial cells were based on the transport of trace amounts of carrier-free radioactive manganese (*14*), and did not distinguish between the two different pools of manganese described here (*20*). To verify our results using an additional

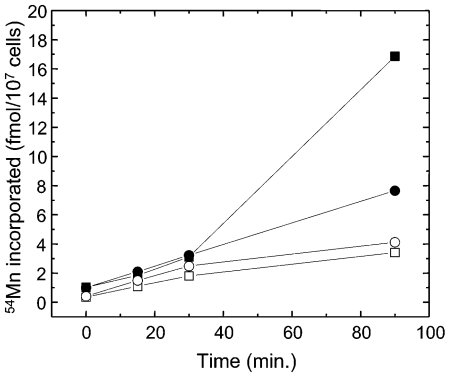

FIGURE 5: Accumulation of radioactive manganese. ^{54}Mn uptake into cells grown in BG11-Mn was measured in the light (squares) and dark (circles). Samples were collected at the indicated times and washed with either 10 mM nonradioactive manganese (filled symbols) or 5 mM EDTA wash buffer (empty symbols).

independent method, we have also performed experiments with radioactive manganese. Using two experimental protocols to stop the accumulation of $^{54}Mn^{2+}$, wash in 10 mM cold manganese, a protocol used in pervious reports (*20*), and in EDTA wash buffer as described above, we could measure the rate of manganese accumulation in the two pools (Figure 5). The EDTA-treated cells represent pool B manganese, while the difference between the cold manganese-washed and the EDTA-washed cells represents pool A. Using the 10 mM cold manganese wash, we were able to show light-dependent uptake of manganese, as reported for pool A in Figure 4A. On the other hand, when the samples were washed with 5 mM EDTA, a slower rate of manganese uptake was measured with no difference between light and dark incubation, similar to the result obtained for pool B in Figure 4C. The data presented in Figure 5 indicate that the exchange rate of the radioactive manganese bound in pool A with the excess cold manganese in the wash solution was slower than the incubation time in the wash solution. Therefore, a large difference in the accumulation of manganese in the light and dark could be observed, similar to that observed for accumulation of manganese in pool A as measured by atomic absorption spectroscopy.

Energetic Requirements for Manganese Accumulation. To determine the source of the light dependence of manganese accumulation, photosynthetic electron flow in *Synechocystis* 6803 was blocked by the specific PSII inhibitor DCMU (*37*). Upon addition of DCMU, manganese accumulation in pool A stopped, and eventually, some of the bound manganese was released (Figure 6). This response is similar to that observed during dark incubation (Figure 4A).

Photosynthetic electron flow generates ATP and NADPH as well as a membrane potential across the thylakoid and, subsequently, cellular membranes. To determine which of these products of photosynthesis is involved in the light-dependent accumulation of manganese, the cells were treated with the proton translocator CCCP that uncouples membrane potentials (*38*). In the short term, CCCP does not affect the levels of ATP and NADPH in the cell (*38*). While inhibition of photosynthetic electron transport by DCMU stopped the accumulation of manganese in pool A, addition of CCCP immediately released all of the manganese in pool A (Figure 7). This release was correlated to the concentration of CCCP in a sigmoidal fashion with 50% of the effect at 0.12 mM

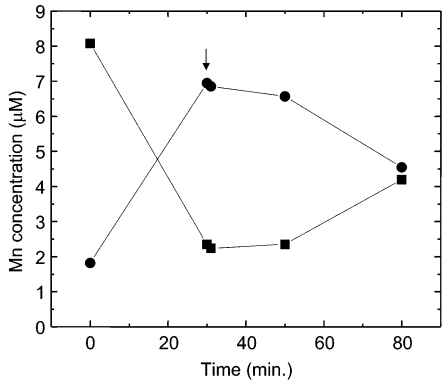

FIGURE 6: Dependence of manganese accumulation on photosynthetic activity. Wild-type cells grown on BG11 medium were tested for manganese accumulation in the light. The arrow indicates addition of 5 μM DCMU: (■) medium and (●) pool A.

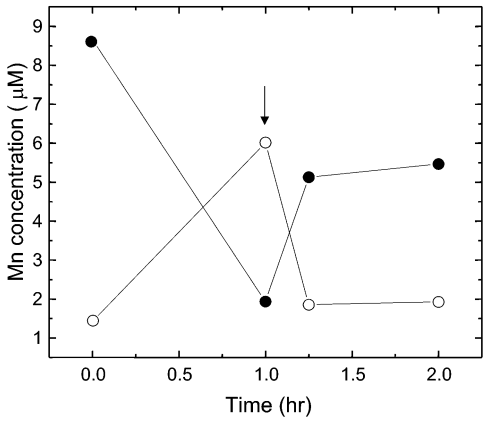

FIGURE 7: Dependence of manganese accumulation on membrane potential. The manganese concentration was measured in the medium (filled symbols) and pool A (empty symbols) in cells grown in BG11. CCCP (0.2 mM) was added at the time indicated by the arrow.

Table 1: Inhibition of Manganese Accumulation by Other Metals[a]

metal	concentration in BG11 (μM)	IC_{50} (mM)
Mg^{2+}	300	1.6
Fe^{3+}	30	0.15
Co^{2+}	0.17	2

[a] Inhibition of the initial rate of manganese transport was measured using a range of metal ion concentrations. Mg^{2+} was added as $MgCl_2$, Fe^{3+} as $FeCl_3$, and Co^{2+} as $CoCl_2$. Initial rates of manganese uptake were fitted by a single-exponential decay function. The first-order rate constants measured at different metal concentrations were plotted as a function of the metal concentration and fitted with a sigmoidal curve. The first-order rate constant in BG11 medium was 0.092 ± 0.03 min^{-1}. The IC_{50} values reflect 50% inhibition of the rate of transport in BG11.

(data not shown). The size of pool B was $2.6 \times 10^6 \pm 4.5 \times 10^5$ atoms/cell throughout the experiment, indicating that CCCP did not compromise the integrity of the inner membrane.

Efficient accumulation of manganese takes place in the BG11 medium that contains many other metal cations that could potentially compete with manganese. This would suggest that the accumulation process is specific to manganese. Indeed, uptake of manganese could be inhibited only by the addition of a vast excess of magnesium or cobalt (Table 1). In addition, 50% inhibition by iron was achieved at a concentration that is 5 times higher than the concentration

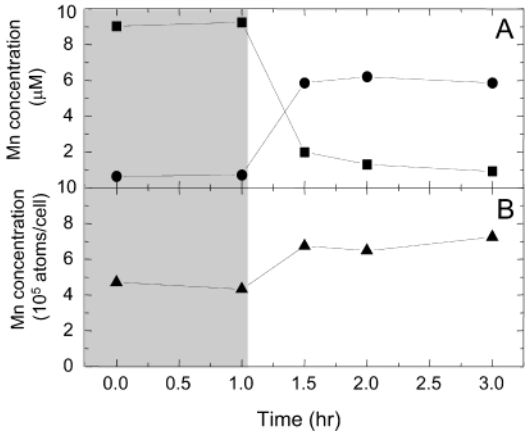

FIGURE 8: Manganese accumulation in the Δ*mntC* mutant. Δ*mntC* cells were grown in BG11 medium and tested for manganese transport using the same experimental protocol as in Figure 4: (A) (■) manganese concentration in the medium and (●) manganese concentration in pool A and (B) (▲) manganese concentration in pool B.

of iron (30 μM) and 16.6 times higher than the concentration of manganese (9 μM) in BG11.

Manganese Accumulation in the Δ*mntC Mutant.* To date, the MntABC transporter is the only manganese transport system that has been described in the cyanobacterium *Synechocystis* sp. PCC 6803 (*19*). This primary transporter operates at low manganese concentrations. To examine the kinetics of manganese transport in cells lacking the MntABC activity, we have used the Δ*mntC* mutant (*19*). As shown in Figure 8A, the kinetics of accumulation of manganese in pool A are similar to those determined for wild-type cells (Figure 4A). However, a difference in the kinetics of manganese accumulation in pool B was observed. The size of pool B in Δ*mntC* cells grown in BG11, at the initial time point, was 4.7×10^5 atoms/cell, 3 times lower than in wild-type cells grown under the same conditions. On the background of this lower concentration, it was easier to measure the activity of additional manganese transporting systems (Figure 8B). Here the transport of manganese into pool B is light-dependent, unlike the situation in wild-type cells grown at a low manganese concentration (Figure 4C), in which MntABC is present.

DISCUSSION

The data presented in this paper reveal the presence of an EDTA washable pool of manganese (pool A) in *Synechocystis* 6803 cells. Cyanobacterial cells can rapidly accumulate manganese from the growth medium into pool A, leaving virtually no free manganese 1 day after dilution into fresh medium. The existence of such a pool has not been described in any other bacterial species.

What is the nature of pool A of manganese? The location of this pool should be in a compartment exposed to EDTA, which can penetrate the outer but not the inner membrane of Gram-negative bacteria (*39*). The ability to porate the outer membrane is correlated to the removal of magnesium and calcium ions that are essential for the integrity of the outer membrane. In accordance with these observations, our data demonstrate that pool A is closely associated with the outer membrane. The manganese in this pool can be bound either to the outer or to the inner face of this membrane. In a

Synechocystis 6803 cells, with a diameter of 2 μm, the concentration of manganese accumulated in pool A, averaged over the entire cell volume, is in the range of 100 mM. However, since pool A manganese is restricted to the envelope layer of the cells, the local manganese concentration should be much higher. The ability to store large concentrations of manganese, and the specificity of the accumulation process, indicate the existence of dedicated manganese storage mechanisms.

Evidence for the molecular nature of this storage mechanism is shown in the XAS data (Figure 3). The XANES data provide clear evidence that the manganese in pool A is present primarily as Mn(II), and suggest that the manganese is present, on average, in a distorted environment. Given the likelihood that the manganese in pool A is present in a heterogeneous mixture of sites, it is difficult to define the manganese environment using a bulk spectroscopy such as EXAFS. However, it is clear that the Mn in pool A is present in an environment that is significantly different from that found for hexaquo Mn(II). The pK_a for $Mn(II)(H_2O)_6$ is approximately 10.5 (*40*). Thus, it is unlikely that the distortions seen in Figure 3 result simply from hydrolysis of bound water molecules. Rather, it is likely that one or more peptide ligands give rise to a nonoctahedral geometry for the Mn(II).

Manganese is not the only metal accumulated in this manner in *Synechocystis* 6803 cells. We have determined that large amounts of iron are bound in an EDTA-extractable pool as well (data not shown). However, only manganese accumulation exhibited a strong light dependence. This dependence is of special interest since the principal sink for manganese in a photosynthetic cell is PSII. Indeed, inhibiting photosynthetic electron flow through PSII stopped the accumulation of pool A manganese. This would imply that the pool is actively maintained at the expense of energy. On the basis of the fast release of manganese in the presence of the uncoupler CCCP, it is likely that the membrane potential is actively involved in maintaining the pool. However, since CCCP collapses any proton gradient across the inner as well as across the thylakoid membrane, a distinction between the potentials across these two membrane systems could not be made during the current study.

A small fraction of the total manganese was not washed out by EDTA (pool B), nor was it released by the addition of DCMU or CCCP. This fraction likely represents a manganese pool internal to the inner membrane. The size of this fraction varies greatly depending on the growth conditions. In the BG11-Mn medium, the concentration of manganese in pool B was 7 times smaller than in the BG11 medium. However, such a decrease did not inhibit photoautotrophic growth, nor did it affect photosynthesis in wild-type *Synechocystis* 6803 cells (*20*). This would imply that under manganese starvation conditions, the cells retain enough manganese for normal photosynthetic activity. The amount of manganese needed for photosynthesis in the cyanobacterial cells can be estimated on the basis of the following: (1) 5−10 μg of chlorophyll/10^8 cells, i.e., $\approx 5 \times 10^7$ chlorophylls/cell, and (2) an average of 500 chlorophylls per electron transfer chain and four manganese ions per PSII, resulting in a manganese concentration in the range of 10^5 atoms/cell in PSII. This indicates that when *Synechocystis* 6803 cells are grown in BG11-Mn, most of the manganese in the cell is associated with PSII. Preliminary results from other photosynthetic bacteria indicate a pool B size in the marine cyanobacterium *Synechococcus* sp. PCC 7002 of 1.5×10^6 atoms/cell, while in the purple bacterium *Rhodobacter capsulatus*, which relies on H_2S rather than H_2O as a source for electrons and lacks the manganese cluster, the pool size is only 1.5×10^4 atoms/cell.

Transport of manganese into pool B was evident only when cells grown in BG11-Mn medium were diluted into BG11 medium. Under manganese starvation conditions, the MntABC transporter is expressed (*20*). We show here that the transport process mediated by this transporter is not light-dependent. In cells grown in BG11, the major process was accumulation in pool A. Very little, if any, manganese transport into pool B could be measured. This does not imply that cells grown in BG11 medium do not have the capacity to transport manganese through the inner membrane. In the Δ*mntC* cells, light-dependent uptake into pool B could be assessed. This manganese transport process, mediated by yet unknown transporter(s), is light-dependent.

Complex strategies had been elucidated for the transport of other transition metals in Gram-negative bacteria, to which analogies can be drawn. The best-described transport system in bacteria is for iron, for which a number of different transport pathways have been described (*41*). These include pathways for transfer of free ferric and ferrous iron as well as pathways for transfers of ferric iron complexed with organic molecules. The activities of a number of these pathways have been demonstrated in *Synechocystis* 6803 (*42*). It is evident from previous work done in this field that the outer membrane serves as a selective barrier for iron, through which transport is mediated by specific active transport systems (*43*). While no data for the accessibility of manganese exist, one may assume that the limitations imposed on iron transport would apply to manganese as well.

On the basis of the results presented here, two working models can be constructed for the pathway of manganese uptake in cyanobacterial cells: (1) manganese is transported in an active, membrane potential-dependent process through the outer membrane and stored in the periplasm (attached to outer membrane) from which it is transferred through the inner membrane in a second transport step, and (2) manganese is stored in a membrane potential-dependent manner on the outer surface of the outer membrane and transported in a concerted manner, across both the outer and the inner membranes, inside the cell.

When cells are in an environment containing little manganese, transport through the inner membrane is mediated by the MntABC transporter in a light-independent but ATP-dependent process. In the presence of high manganese concentrations, the cells bind as much manganese as possible in the envelope layer, to be used when the cells divide and the external manganese concentration decreases. The 80-fold excess of stored manganese should last for at least six rounds of cell division. Since the generation time of these cyanobacterial cells is ~10 h, this assumption would fit nicely with the 3 days it takes for cells transferred to BG11-Mn medium to develop the manganese starvation characteristics (unpublished observation). The periplasmic binding of manganese prevents the potential harmful effects of manganese inside the cell. The accumulated manganese is then

transported into the cell at a slow rate which is limited by the internal need for manganese.

ACKNOWLEDGMENT

We thank Prof. T. J. Kappock and members of the Pakrasi lab group for collegial discussions.

REFERENCES

1. Frausto de Silva, J. J. R., and Williams, R. J. P. (2001) *The Biological Chemistry of the Elements*, 2nd ed., Oxford University Press, Oxford, U.K.
2. O'Halloran, T. V., and Culotta, V. C. (2000) *J. Biol. Chem. 275*, 25057−25060.
3. Liochev, S. I., and Fridovich, I. (1999) *IUBMB Life 48*, 157−161.
4. Pena, M. M., Lee, J., and Thiele, D. J. (1999) *J. Nutr. 129*, 1251−1260.
5. Hantke, K. (2001) *Curr. Opin. Microbiol. 4*, 172−177.
6. Moncrief, M. B., and Maguire, M. E. (1999) *J. Biol. Inorg. Chem. 4*, 523−527.
7. Jakubovics, N. S., and Jenkinson, H. F. (2001) *Microbiology 147*, 1709−1718.
8. Tseng, H. J., McEwan, A. G., Paton, J. C., and Jennings, M. P. (2002) *Infect. Immun. 70*, 1635−1639.
9. Silver, S., and Kralovic, M. L. (1969) *Biochem. Biophys. Res. Commun. 34*, 640−645.
10. Eisenstadt, E., Fisher, S., Der, C.-L., and Silver, S. (1973) *J. Bacteriol. 113*, 1363−1372.
11. Perry, R. D., and Silver, S. (1982) *J. Bacteriol. 150*, 973−976.
12. Jasper, P., and Silver, S. (1978) *J. Bacteriol. 133*, 1323−1328.
13. Cheniae, G. M., and Martin, I. F. (1967) *Biochem. Biophys. Res. Commun. 28*, 89−95.
14. Silver, S., and Jasper, P. (1977) in *Microorganisms and Minerals* (Weinberger, E. D., Ed.) pp 105−149, Marcel Dekker, Inc., New York.
15. Culotta, V. C. (2000) *Met. Ions Biol. Syst. 37*, 35−56.
16. Hillier, W., and Babcock, G. T. (2001) *Plant Physiol. 125*, 33−37.
17. Yachandra, V. K., Sauer, K., and Klein, M. P. (1996) *Chem. Rev. 96*, 2927−2950.
18. Gantt, E. (1994) in *The Molecular Biology of Cyanobacteria* (Bryant, D. A., Ed.) pp 119−138, Kluwer, Dordrecht, The Netherlands.
19. Bartsevich, V. V., and Pakrasi, H. B. (1995) *EMBO J. 14*, 1845−1853.
20. Bartsevich, V. V., and Pakrasi, H. B. (1996) *J. Biol. Chem. 271*, 26057−26062.
21. Allen, M. M. (1968) *J. Phycol. 4*, 1−4.
22. Zak, E., Norling, B., Andersson, B., and Pakrasi, H. B. (1999) *Eur. J. Biochem. 261*, 311−316.
23. Murata, N., and Omata, T. (1988) *Methods Enzymol. 167*, 245−251.
24. McMaster, W. H., Del Grande, N. K., Mallett, J. H., and Hubbell, J. H. (1969) U.S. Department of Commerce Report Number UCRL-50174-SEC 2-R1, U.S. Government Printing Office, Washington, DC.
25. Newville, M. (2001) *J. Synchrotron Radiat. 8*, 322−324.
26. http://cars9.uchicago.edu/ifeffit/.
27. Zabinsky, S. I., Rehr, J. J., Ankudinov, A., Albers, R. C., and Eller, M. J. (1995) *Phys. Rev. 52*, 2995−3009.
28. Rehr, J. J., Mustre, d. L. J., Zabinsky, S. I., and Albers, R. C. (1991) *J. Am. Chem. Soc. 113*, 5135−5140.
29. Ankudinov, A., Ravel, B., Rehr, J. J., and Conradson, S. (1998) *Phys. Rev. 58*, 7565−7576.
30. Martel, A. E. (1964) *Stability constants*, Vol. 17, The Chemical Society, London.
31. Hancock, R. E. (1984) *Annu. Rev. Microbiol. 38*, 237−264.
32. Fulda, S., Mikkat, S., Schroder, W., and Hagemann, M. (1999) *Arch. Microbiol. 171*, 214−217.
33. Webb, E. A., Moffett, J. W., and Waterbury, J. B. (2001) *Appl. Environ. Microbiol. 67*, 5444−5452.
34. Riggs-Gelasco, P. J., Mei, R., Yocum, C. F., and Penner-Hahn, J. E. (1996) *J. Am. Chem. Soc. 118*, 2387−2399.
35. Stemmler, T. L., Sossong, T. M., Goldstein, J. I., Ash, D. E., Elgren, T. E., Krutz, D. M., and Penner-Hahn, J. E. (1997) *Biochemistry 36*, 9847−9858.
36. Liu, W. T., and Thorp, H. H. (1993) *Inorg. Chem. 32*, 4102−4105.
37. Rutherford, A. W., and Krieger-Liszkay, A. (2001) *Trends Biochem. Sci. 26*, 648−653.
38. Nicholls, D. G., and Ferguson, S. J. (1982) *Bioenergetics 2*, Academic Press, London.
39. Vaara, M. (1992) *Microbiol. Rev. 56*, 395−411.
40. Perrin, D. D. (1969) *Dissociation constants of inorganic acids and bases in aqueous solution*, Butterworths, London.
41. Braun, V., and Killmann, H. (1999) *Trends Biochem. Sci. 24*, 104−109.
42. Katoh, H., Hagino, N., Grossman, A. R., and Ogawa, T. (2001) *J. Bacteriol. 183*, 2779−2784.
43. Braun, V. (1995) *FEMS Microbiol. Rev. 16*, 295−307.

BI026892S